Dynamic Mechanical Properties of Styrene-Butadiene Composites Reinforced by Defatted Soy Flour and Carbon Black Co-Filler

L. Jong

United States Department of Agriculture, National Center for Agricultural Utilization Research, Agricultural Research Service, 1815 North University Street, Peoria, Illinois 61604

Received 15 December 2006; accepted 22 July 2007
DOI 10.1002/app.27105
Published online 21 December 2007 in Wiley InterScience (www.interscience.wiley.com).

ABSTRACT: Carboxylated styrene-butadiene (SB) composites reinforced by a mixture of defatted soy flour (DSF) and carbon black (CB) were investigated in terms of their dynamic mechanical properties. DSF is an abundant renewable commodity and has a lower cost than CB. DSF contains soy protein, carbohydrate, and whey. Aqueous dispersions of DSF and CB were first mixed and then blended with SB latex to form rubber composites using freeze-drying and compression molding methods. At 140°C, a single filler composite reinforced by 30% DSF exhibited roughly a 230-fold increase in the shear elastic modulus compared to the unfilled SB rubber, indicating a significant reinforcement effect by DSF. Mixtures of DSF and CB at three different ratios were investigated as co-fillers. Temperature sweep experiments indicate the shear elastic moduli of the co-filler composites are between that of DSF and CB composites. Strain sweep experiments were used to study the fatigue and recovery behaviors of these composites. Compared with the DSF composites, the recovery behaviors of the 30% co-filler composites after the eight consecutive deformation cycles of dynamic strain were improved and similar to that of 30% CB composite. Strain sweep experiments also indicated that the co-filler composites have a greater elastic modulus than the CB reinforced composites within the strain range measured. J Appl Polym Sci 108: 65–75, 2008

Key words: biomaterials; composites; reinforcement; mechanical properties; rubber

INTRODUCTION

Rubber material needs to be reinforced with fillers and subsequently crosslinked with crosslinking agents in order to obtain a sufficient modulus for practical applications. Carbon black derived from aromatic oil in petroleum or from natural gas is the most common reinforcing filler. Substitution of carbon black with renewable fillers has been investigated in recent years. Recent studies have reported the modulus enhancement of rubbers by natural materials, for example, soybean products,[1–4] oil palm wood,[5] crab shell chitin,[6] and bamboo fiber.[7] The use of renewable protein in rubber latex to form composites was also reported in a few patents[8–10] and can be traced back to the 1930s. For example, Lehmann et al. demonstrated the use of casein (milk protein) in natural rubber latex to achieve approximately a fourfold increase in the modulus.[10] Protein as an additive in rubber materials has also been claimed to improve the anti-skid resistance of winter tread tires.[11–13] In rubber reinforcement, factors such as aggregate structure, effective filler volume fraction, filler–rubber interaction and the elastic modulus of filler clusters all have an important impact on the moduli of rubber composites.[14] Mechanically, the elastic modulus of base rubber is not significant when compared with the modulus of the filler network in highly filled elastomeric composites.[15] For some of practical applications, the issue of moisture sensitivity is always associated with natural materials, but it may be improved through product formulation and/or selective applications. For example, they may be used as components in multi-layered structures, in coated objects, in elevated temperature applications, or as rubber parts formulated with hydrophobic plasticizer.

DSF is the soy product remaining after soybean oil is removed from soybean flakes. It is an abundant and inexpensive renewable commodity. The composition of defatted soy flour includes soy protein, soy carbohydrate (insoluble carbohydrate), and soy whey (soluble carbohydrate).[16] DSF has a lower raw material cost than carbon black. Previously, DSF was used to reinforce styrene-butadiene rubber and

Names are necessary to factually report on available data; however, the USDA neither guarantees nor warrants the standard of the product, and the use of the name by USDA implies no approval of the product to the exclusion of others that may also be suitable.

Correspondence to: L. Jong (lei.jong@ars.usda.gov).

showed a significant reinforcement effect in the small strain region.[1] The objective of this investigation is to investigate the co-filler effect by using a mixture of DSF and CB as reinforcement fillers.

The rubber matrix used in this study is a styrene-butadiene (SB) rubber with a small amount of carboxylic acid containing monomer units. The carboxylated SB forms a crosslinked rubber by the aggregation of ionic functional groups without the complication of covalent reactions. Carboxylated SB rubber is classified as an ion-containing polymer. Its viscoelastic properties are affected by molecular weight, degree of crosslinking, glass transition temperature (T_g), copolymer composition, the number of ionic functional groups, the size of ionic aggregation, the degree of neutralization, and the size of the neutralizing ions.[17,18] The film structures of carboxylated latexes also showed a honeycomb-like pattern due to a higher concentration of carboxylic acid groups on the particle surface.[19] For filler–matrix interactions,[15] soy protein contains a significant amount of carboxylic acid and substituted amine groups[20] to interact with the polymer matrix. Soy carbohydrates can also interact with carboxylic functional groups in the SB matrix through hydrogen bonding and ionic interactions. Structurally, soy protein is a globular protein and its aggregate is similar to colloidal aggregates, but soy carbohydrate is a non-globular, film-like material.[1,2] Although ionic interactions can occur between these soy products and carboxylated SB, the condensation reactions do not occur under alkali conditions between the carboxyl groups of SB and the major functional groups such as hydroxyl, carboxyl, thiol, amine, and amide groups in DSF.

EXPERIMENTAL

Materials

The defatted soy flour (Nutrisoy 7B) used in this research was a spray dried powder (Archer Daniels Midland Company, Decatur, IL). The DSF contained $\sim$ 53% soy protein and had a protein dispersibility index (PDI) of $\sim$ 90. Sodium hydroxide, used to adjust pH, was ACS grade. Aqueous dispersions of carbon black N-339 (Sid Richardson Carbon Co., Fort Worth, TX) were prepared by dispersing $\sim$ 100 g of carbon black (CB) in water with the aid of a surfactant, sodium lignosulfonate (Vanisperse CB, Lignotech USA, Rothschild, WI). The weight fraction of the surfactant based on carbon black is 3%. The dispersion was homogenized at 10^4 rpm for 1 h. The resulting CB dispersion had a solid content of 12.7%. The carboxylated styrene-butadiene (SB) latex was a random copolymer of styrene, butadiene, and small amount of carboxylic acid containing monomers (CP 620NA, Dow Chemical Company, Midland, MI). The glass transition temperature of carboxylated SB Latex is $\sim$ 10°C as determined by differential scanning calorimetry. The styrene/butadiene ratio estimated from the glass transition temperatures of a series of commercially available carboxylated styrene butadiene (Mallard Creek Polymers, Charlotte, NC) was $\sim$ 65/35. The dried latex is not known to be soluble in any solvent or combination of solvents. The latex received had $\sim$ 50% solids and a pH $\sim$ 6. The volume weighted mean particle size of the latex was $\sim$ 0.18 μm.

Preparation of elastomer composites

In this study, freeze-drying and compression molding methods were used instead of a casting method because there is a density difference between DSF and CB. Using a casting method may produce a less homogeneous sample due to different precipitation rates of DSF and CB. DSF was first dispersed in water at $\sim$ 10% concentration, pH $\sim$ 10, and 55°C for 1 h. The cooled DSF dispersion was then blended homogeneously with carbon black dispersion at three different dry weight ratios (1 : 3, 1 : 1, and 3 : 1). The SB latex, previously adjusted to pH 9, was then added to the filler mixture and mixed homogeneously to form composites with three different filler contents (10, 20, and 30 wt %). The homogeneous composite mixtures were then quickly frozen in a rotating shell freezer at about −40°C, followed by freeze-drying in a freeze-dryer (LABCONCO, Kansas City, MO). The moisture content of dried composite crumb is less than 2%. The freeze-dried crumb was then compression molded in a plunge type mold at 69 MPa and 140°C for 2.5 h. After compression molding, the samples were relaxed and further annealed at 95, 110, and 140°C for 24 h, respectively. The annealing is used to dry the samples because moisture behaves as a plastiscizer for DSF and has an effect on composite moduli. The torsion bars of 100% carboxylated SB rubber and DSF were also prepared using the same process as that of the co-filler composites. The dried samples had moisture content less than 0.8% as measured by halogen moisture analyzer (Mettler Toledo HR73) at 105°C for 60 min. For comparison, DSF and CB composites were prepared by using the same procedure as that of co-filler composites. The densities of DSF, CB, and SB were measured by using a density bottle (Gay-Lussac bottles) with a low viscosity poly(dimethylsiloxane) as the immersion liquid.

Dynamic mechanical measurements

A Rheometric ARES-LSM rheometer (TA Instruments, Piscataway, NJ) with TA Orchestrator software v 7.1.2.3 was used for the dynamic mechanical

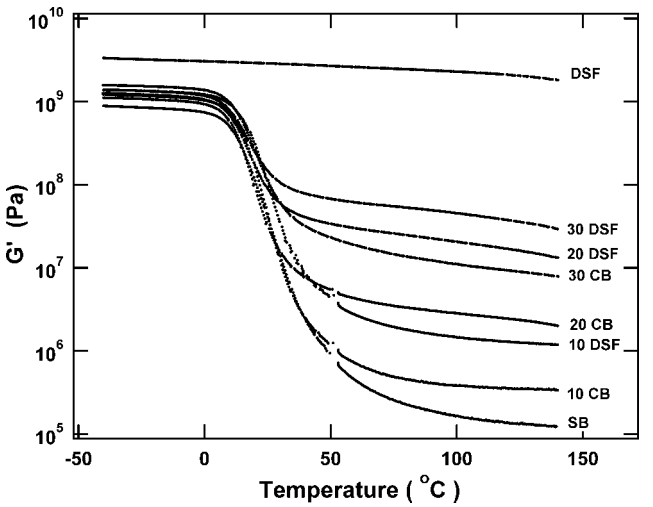

Figure 1 Storage moduli of DSF/SB and CB/SB composites. The weight fraction of filler is shown at the end of each curve.

measurements. To study thermal mechanical properties of the composites, temperature ramp experiments were conducted using torsion rectangular geometry with a heating rate of 1°C/min in a temperature range from −70°C to 140°C. When using torsion rectangular geometry, torsional bars with dimensions of ~ 40 mm × 12.5 mm × 5 mm were mounted between a pair of torsion rectangular fixtures and the dynamic mechanical measurements were conducted at a frequency of 0.16 Hz (1 rad/s) and a strain of 0.05%.

To study the stress softening effect, strain sweep experiments were conducted using a torsional rectangular geometry to measure the oscillatory storage and loss moduli, G′(ω) and G″(ω). The shear strain-controlled rheometer is capable of measuring the oscillatory strain down to 3×10^{-5}% strain (TA Instruments, Piscataway, NJ). The rheometer was calibrated in terms of torque, normal force, phase angle, and strain using the instrument's standard procedure. A rectangular sample with dimension of ~ 12.5 mm × 20 mm × 5 mm was inserted between the top and bottom grips. The gap between the fixtures was ~ 7 mm in order to achieve a strain of ~ 14%. A sample length shorter than 5 mm is not desirable because of the resulting shape change from the clamping at both ends of the sample. The frequency used in the measurements was 1 Hz. The oscillatory storage and loss moduli were measured over a strain range of

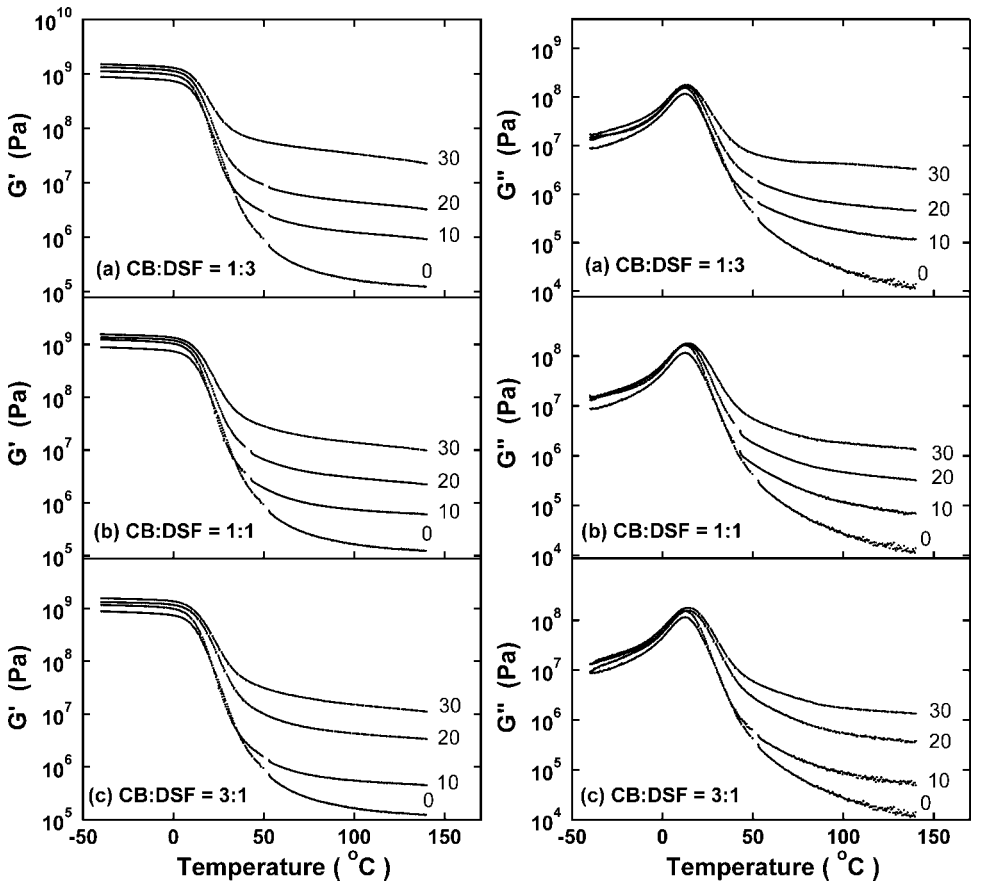

Figure 2 Elastic and loss moduli of co-filler composites. The weight fraction of co-filler is indicated at the end of each curve. The co-filler ratios are shown on the graphs.

$\sim$ 0.007%–14%. The actual strain sweep range is limited by sample geometry and motor compliance at large strain, and transducer sensitivity at small strain. The data that was out of the transducer range was rejected. Although harmonics in the displacement signal may be expected in a nonlinear material, a previous study[21] indicated that the harmonics are not significant if the shearing does not exceed 100%. Each sample was conditioned at 140°C for 30 min to reach an equilibrated dimension and then subjected to eight cycles of dynamic strain sweep in order to study the stress softening effect. The delay between strain cycles was 100 s. For clarity, only data from the first, fourth, and eighth cycles are presented in the figures. To measure the recovery curves, the samples that had been subjected to the eight strain cycles were allowed to recover at 140°C for 24 h before they were subjected to one cycle of strain sweep.

RESULTS AND DISCUSSION

Thermal mechanical properties of single-filler composites

Figure 1 shows the elastic moduli of single-filler composites. Previous studies[4] indicated that soy protein and CB reinforced composites had a percolation transition at less than 8 wt % filler fraction, above which a logarithmic plot of modulus vs. filler fraction is linear. For the current system of soy protein and carbohydrates, it is likely that the range of filler fractions in the composites is also above the percolation threshold, which means the fillers can form a network due to the presence of a sufficient number of filler aggregates in the rubber matrix. At 140°C, the 30% DSF composite has a G′ of 29.35 MPa compared to 0.124 MPa for the G′ of SB. The significant increase 230-fold of G′ is most likely due to the rigid filler network of the DSF (Fig. 1) and possibly also a contribution from the immobilized polymer matrix. For all filler fractions, DSF composites have a significantly greater G′ than CB composites within the rubber plateau region. The comparison is based on the weight fraction of filler, which is relevant to the economic value of the filler. DSF has a density of 1.41 gm/cm^3 and CB has a density of 1.73 gm/cm^3. Therefore, DSF has a greater volume fraction than CB at the same weight fraction and the reinforcement effect is proportional to the volume fraction instead of the weight fraction when other factors are equal. These other factors, including the aggregate size of the filler, filler–filler interactions, and filler–rubber interactions, also contribute to the observed modulus behavior. The number average size of dry DSF is $\sim$ 6 μm after correcting for the swelling effect in water. The number average size of CB aggregates[4] is $\sim$ 0.3 μm. When other factors are equal, a filler with smaller particle size generally gives rise to a greater reinforcement effect. However, the stronger DSF composites are mainly due to the formation of a stronger DSF filler network. Similar trends in the aggregate sizes and filler–filler interactions of other soy-fillers were also observed previously.[1,4] It is interesting to note that the 20% DSF composite has a greater G′ than the 30% CB composite. The 20% DSF composite also has a smaller volume fraction than the 30% CB composite. This indicates that DSF can form a stronger filler-related network structure in the carboxylated styrene-butadiene matrix.

It is also noted that the reinforcement effect in these freeze-dried samples is less than that prepared

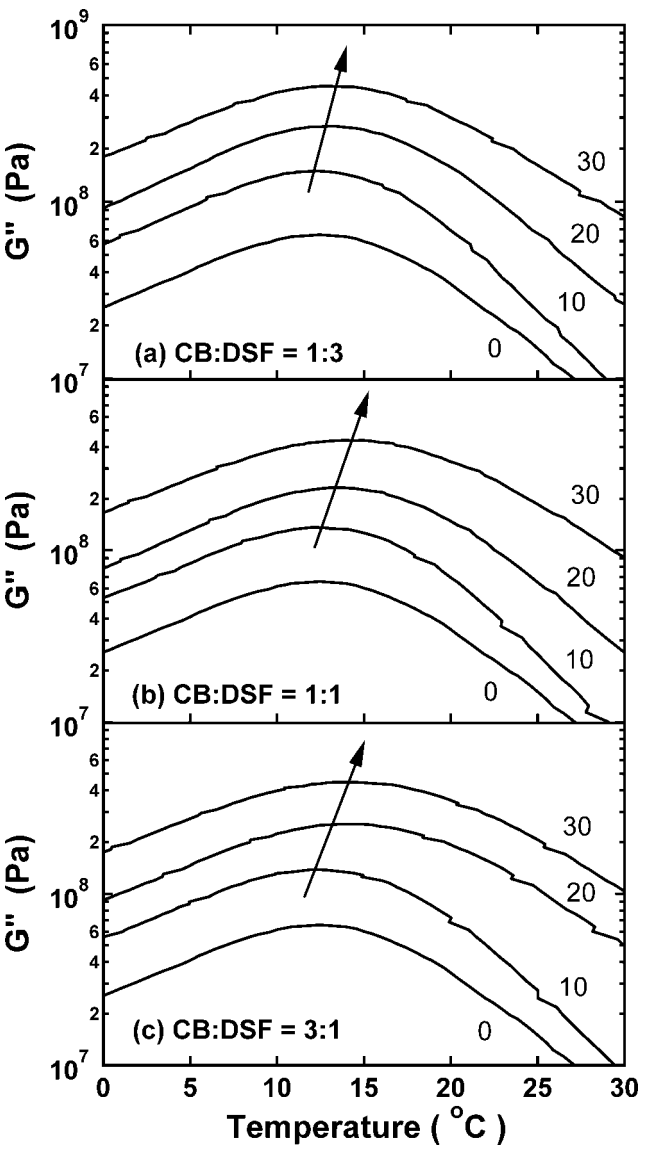

Figure 3 Loss moduli of co-filler composites. The weight fraction of co-filler is shown at the end of each curve. The curves are vertically shifted to give a clearer view. The co-filler ratios are shown on the graphs. The trend of shifting in G″ maximum is indicated by an arrow.

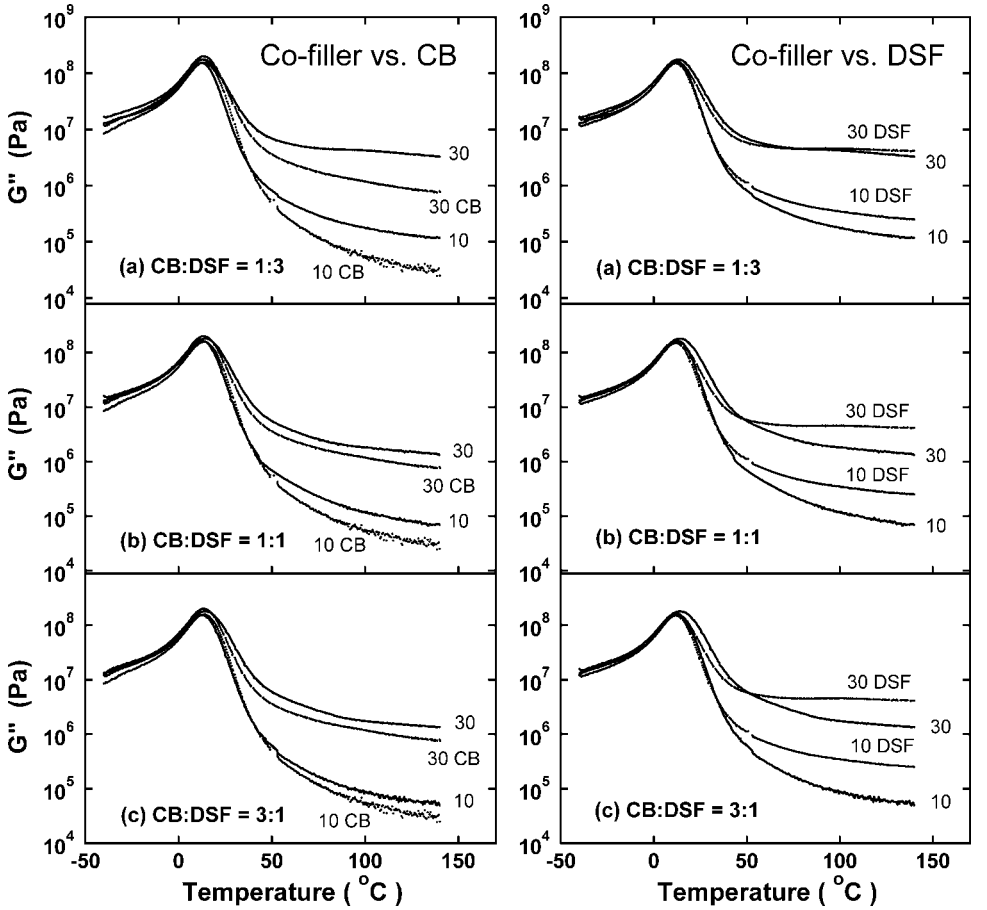

Figure 4 Loss moduli of co-filler and single filler composites. The weight fraction of co-filler is shown at the end of each curve. The weight fraction and filler type of single filler composites are also shown near their curves. The co-filler ratios are also shown on the graphs.

by a casting method reported previously[1] due to the difference in their composite structures. In a previous study,[1] the samples prepared by the casting method were dried at 75°C for 72 h and annealed at 110 and 140°C for 24 h, respectively. The greater G′ in composites prepared by the casting method instead of the freeze-drying method can be explained by the strength of the filler network. The casting method is a slow process which allows the fillers to associate with each other as water evaporates, similar to the phase separation phenomenon in polymer blends. The freeze-drying method, on the other hand, produces a homogeneous mixture of filler and rubber particles by freezing them in a short period of time, where the filler aggregates are surrounded by the rubber particles because the filler has a smaller volume fraction in the mixture. Upon compression molding of freeze-dried crumbs, the filler network structure is more likely to have a polymer region sandwiched between filler aggregates compared to the filler network structure produced by the casting method. With the same filler, filler aggregate size, and filler volume fraction, a filler network with more polymer regions between filler aggregates is softer than a filler network without polymer mediation. Therefore, the polymer mediation model[22] is adequate in explaining these differences. Another potential variable is that the composites prepared by the freeze-drying method may have a thicker polymer region between filler aggregates and thus have a softer filler network structure because the rigid immobilized polymer layer is likely to extend only a few nanometers[23] outward from the filler surface.

Thermal mechanical properties of co-filler composites

Figure 2 shows elastic and loss moduli of co-filler composites at three different co-filler ratios. The general features of G′ over the entire temperature range for the three different co-filler ratios are similar and can be understood from the G′ of their individual components shown in Figure 1. G″ of co-filler composites are shown in Figures 2 and 3. Small shifts of less than 2°C towards a higher temperature are seen in the mixtures of G″ as the filler concentration increases. The shifting of G″ maximums to a higher

temperature as the filler concentration increases are less than 2°C. Although the extent of shifting is small, the trend to shift with the increasing co-filler content is clear and it appears to shift more in the composites with higher CB content. This may indicate that the smaller size of the carbon black aggregates does have some effect in increasing the fraction of immobilized polymer chains. Figure 4 shows that the comparison of G″ maxima of the co-filler and single filler composites. For the 10% composites, there is not much difference in the width of the loss maxima. But, for the 30% composites, the co-filler composites have a broader G″ maxima than either CB or DSF single filler composites, especially on the high temperature side of the peak. This indicates that there are different relaxation modes of the polymer matrix because different parts of the polymer matrix are immobilized by the co-fillers to a different extent. The damping behaviors of these co-filler composites are shown in Figure 5. It follows the general trend of decreasing value as the filler concentration is increased. In the rubbery region, the tan δ values at 140°C are similar for all co-filler composites and are within the range of 0.11–0.14, which is slightly higher than the tan δ values (0.07–0.10) of the carbon black composites shown in Figure 6. In the glass transition region, the tan δ values of co-filler composites are greater than that of DSF composites, but smaller than that of CB composites, similar to the relationship observed in their G′ values. The magnitude of tan δ has practical importance in some rubber applications. For example, in tire applications, a rubber composite that has a smaller tan δ value tends to have a reduced rolling resistance and save energy, while a larger tan δ tends to have an improved skid resistance and wet grip. The ability of DSF to absorb some moisture in a wet state tends to reduce G′ and increase tan δ, leading to better wet traction.

For practical purposes, the G′ of all co-filler reinforced composites are summarized in Figure 7. The elastic moduli of co-filler composites are within the boundaries set by the DSF and CB composites. Compared to CB composites prepared by the same procedure, all co-filler composites showed a greater elastic modulus in the rubber plateau region. This indicates that the substitution of CB with more economical DSF leads to an increase in the elastic modulus of the composite, but with a reduced filler cost. Comparing with DSF composites, the co-filler reinforced composites have a lower elastic modulus, but they have a better recovery behavior due to the presence of CB. The recovery behavior of these composites will be discussed in their stress softening effect. For 10% composites in Figure 7, the G′ values of co-filler composites increase directly with DSF content, likely due to a stronger DSF related filler network structure. However, for the 20 and 30% composites, there is no simple trend, possibly due to a more complicated nature of co-filler complexes.

Fatigue and recovery

The stress softening effect of co-filler composites is shown in Figure 8. The retention of G′ in the small strain region can be used to evaluate the instant recovery behavior after the eight cycles of strain deformation. Thus, the G′ at 0.05% strain in the eighth cycle of the composites shown in Figure 8(a,b,c) retains 72%, 69%, and 70% of their first cycles, respectively. Comparing with the retention of ~ 60% G′ for the DSF composite and ~ 71% G′ for the CB composite, co-filler reinforced composites show a similar G′ retention to that of the CB composites.

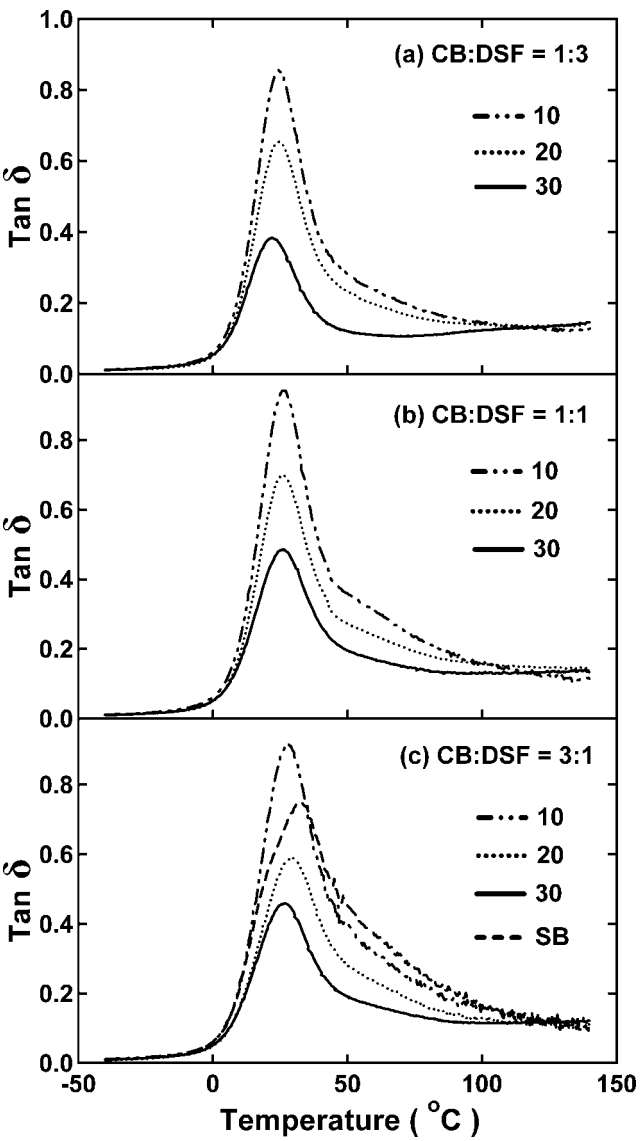

Figure 5 Loss tangent of the co-filler composites. The weight fractions of the co-fillers and the co-filler ratios are shown on the graphs.

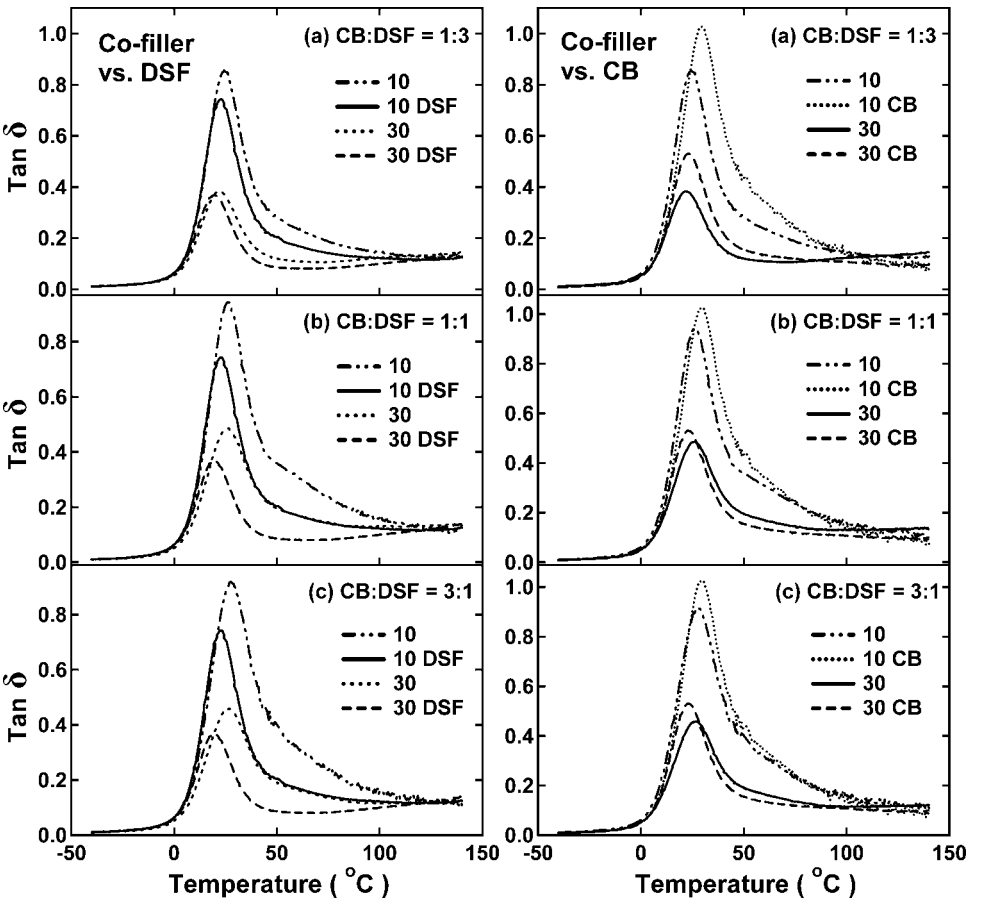

Figure 6 Loss tangent of co-filler composites. The weight fractions of the co-fillers and the co-filler ratios are shown on the graphs. The weight fraction and filler type of single filler composites are also indicated.

In addition to the instant recovery behavior, strain-dependent recovery moduli were also measured after the deformed composites were reconditioned at 140°C for 24 h. These recovery curves are identified in Figures 8, 9, and 10 as R. About 30% co-filler composite with 1 : 3 co-filler ratio recovered 87% of its initial modulus and is about the same as that of 30% CB composite. 1 : 1 and 3 : 1 co-filler composites with 30% filler content also show a total recovery of G′ after reconditioning. The recovery curves in Figure 8 also indicate that the composites with a higher concentration of CB tend to have better recovery behavior. In addition, the moduli of recovery curves for both 1 : 1 and 3 : 1 composites exceeded the moduli of their first strain cycles. This is an indication that the samples prepared by the freeze-drying method are in a homogeneous state, but are not necessarily in an equilibrium state. The perturbation of composite structure by the strain cycles appears to cause the filler structure to rearrange and form a slightly stronger structure through the improved connectivity between filler aggregates.

For loss modulus under consecutive strain cycles, the energy dissipation processes of 1 : 3, 1 : 1, and 3 : 1 co-filler composites (Fig. 8) became less pronounced and their maxima were shifted from ~ 1.2% strain, 0.52% strain, and 0.5% strain to ~ 1.1% strain, 0.33% strain, and 0.19% strain, respectively. It appears that the extent of shifting increases directly with the CB content in the co-filler composites. The structure responsible for the energy dissipation process is obviously reduced after the first three cycles. A loss maximum of a composite that occurs at a larger % strain indicates a more elastic structure, which requires a greater extent of deformation to break down the filler related structure. It is also noted that G′ maximums occur in the small strain region in Figure 8. These G′ maximums are similar to the previous observation on the soy protein filled rubber composites.[4]

For 20% co-filler composites (Fig. 9), the elastic moduli and recovered G′ behave similarly to that of 30% co-filler composites. To further analyze the major contribution of this behavior, the strain dependent behaviors of the composites with 20% DSF or CB filler were measured and shown in Figure 10. Figure 10(a) shows that the recovery curve of the DSF composite did not exceed the G′ of the first cycle, but Figure 10(b) shows that the recovery curve of the CB composite exceeds the G′ of the first cycle.

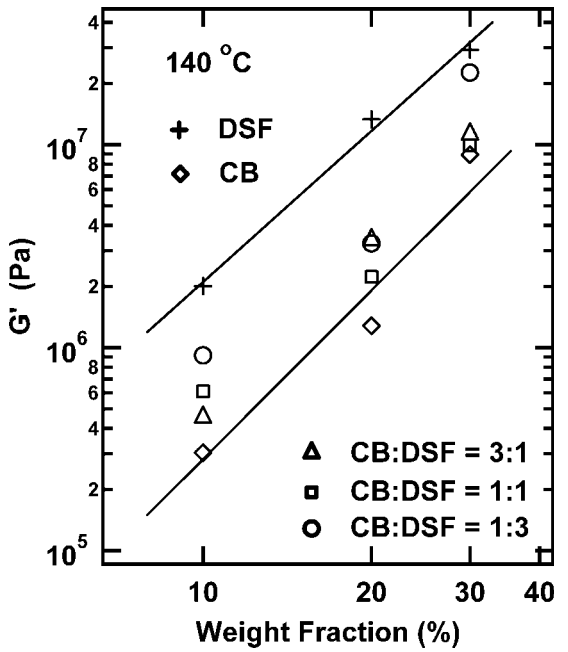

Figure 7 Elastic moduli of co-filler composites at 140°C. The DSF and CB composites are also included for comparison.

This is an indication that CB is responsible for the structure rearrangement in the co-filler composites. The observation is likely due to the ability of smaller CB aggregates to diffuse in a softer rubber matrix and form a more connected filler related network.

For the loss tangent properties at 140°C, the magnitude of tan δ for the co-filler composites roughly follows the additive rule of individual fillers, where tan δ decreases as the CB content is increased in the composites.

Reversible strain-dependent behavior

Payne[24–26] reported the reduction of shear elastic modulus with increasing strain on carbon black filled rubbers in the early 1960s. Later Kraus[27] proposed a phenomenological model based on Payne's postulation of filler networking. The model is based on the aggregation and de-aggregation of carbon black agglomerates. In this model, the carbon black contacts are continuously broken and reformed under a periodic sinusoidal strain. Based on this kinetic aggregate forming and breaking mechanism at equilibrium, elastic modulus was expressed as follows:

$$\frac{G'(\gamma) - G'_\infty}{G'_0 - G'_\infty} = \frac{1}{1 + (\gamma/\gamma_c)^{2m}} \quad (1)$$

where G'_∞ is equal to $G'(\gamma)$ at very large strain, G'_0 is equal to $G'(\gamma)$ at very small strain, γ_c is a characteristic strain where $G'_0 - G'_\infty$ is reduced to half of its zero-strain value, and m is a fitting parameter related to filler aggregate structures. Equation (1) has been shown to describe the behavior of $G'(\gamma)$ in carbon

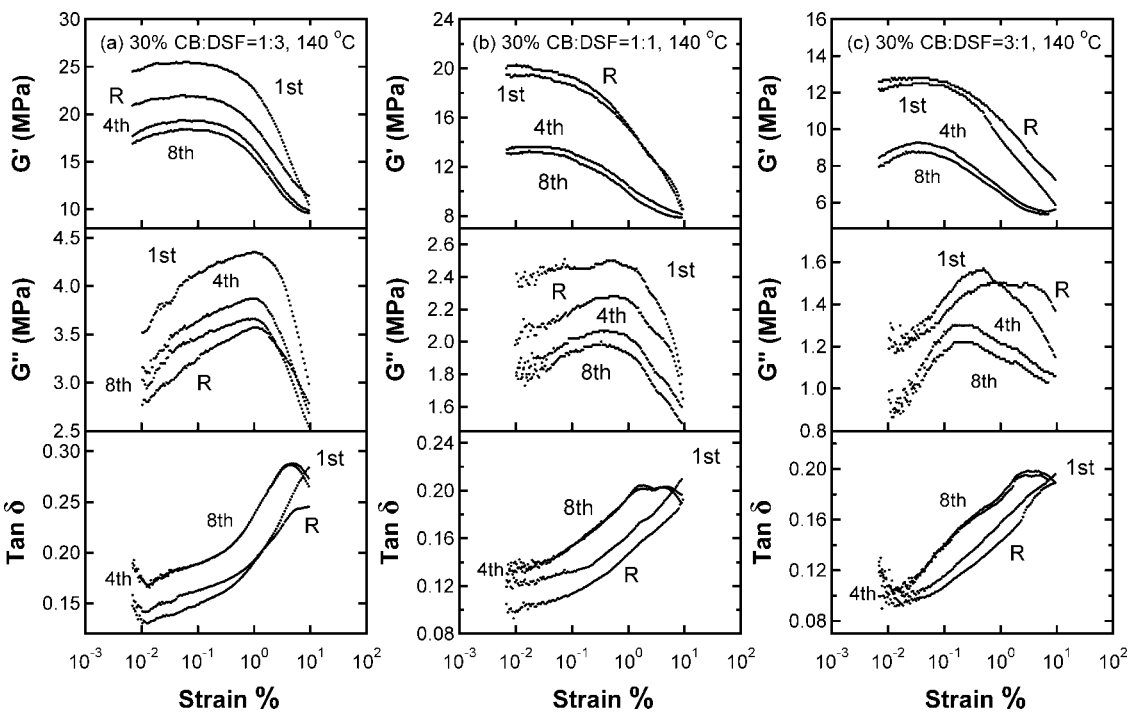

Figure 8 Strain sweep experiments of composites reinforced by 30 wt % co-filler at 140°C. Co-filler ratios are shown on the graphs. Only the 1st, 4th, and 8th strain cycles are shown. R indicates the recovery curve after the samples were conditioned at 140°C for 24 h.

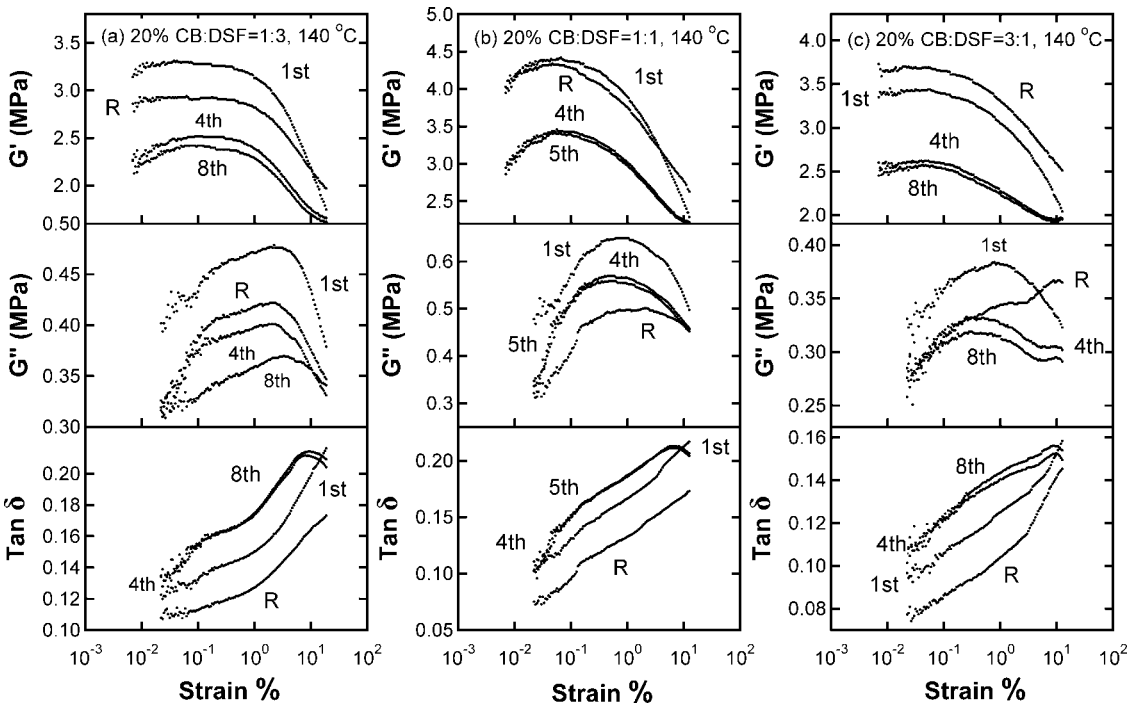

Figure 9 Strain sweep experiments of composites reinforced by 20 wt % co-filler at 140°C. Co-filler ratios are shown on the graphs. Only the 1st, 4th, and 8th strain cycles are shown. R indicates the recovery curve after the samples were conditioned at 140°C for 24 h.

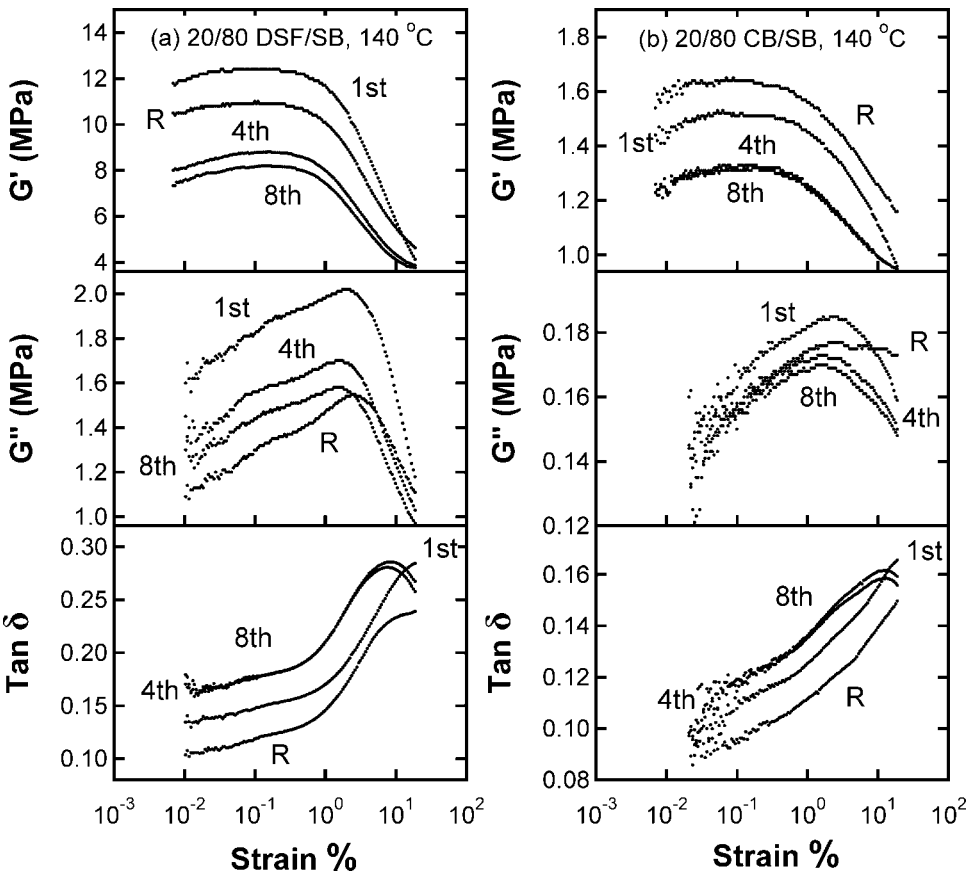

Figure 10 Strain sweep experiments of composites reinforced by 20 wt % filler prepared by the freeze-drying method: (a) DSF composite; (b) CB composite. Only the 1st, 4th, and 8th strain cycles are shown. R indicates the recovery curve after the samples were conditioned at 140°C for 24 h.

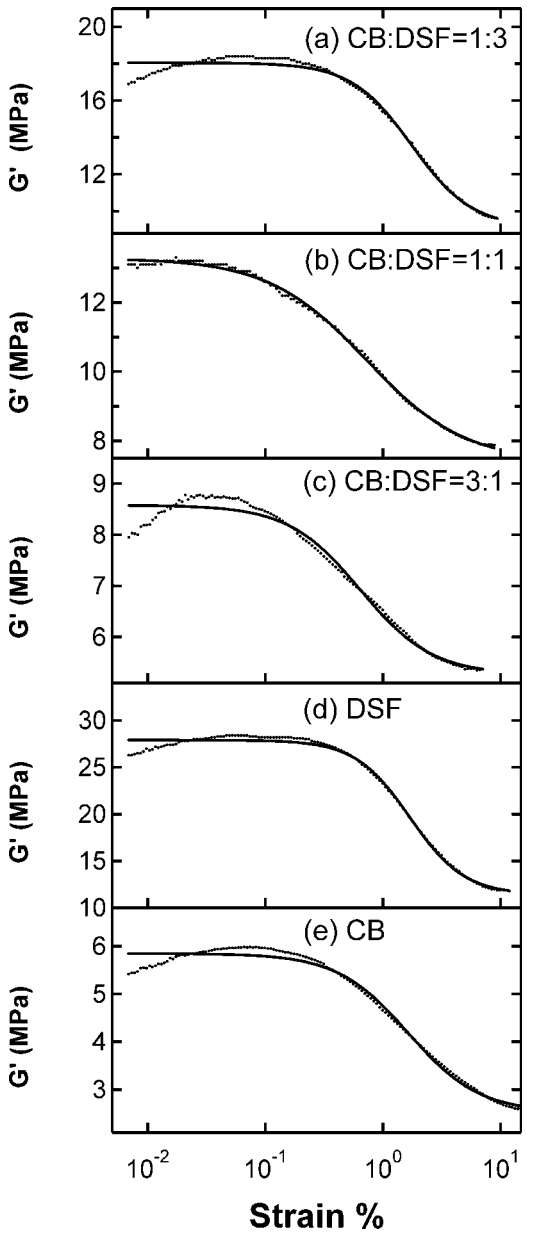

Figure 11 The composites with 30% filler. The 8th cycle of strain sweep experiments at 140°C and 1 Hz. Solid lines are the fit from the Kraus model.

black filled rubber reasonably well.[14] The loss modulus and loss tangent, however, do not have good agreement with experiments,[28] mainly due to the uncertainty in the formulation of a loss mechanism.

The physical meaning of m in the Kraus model may be obtained from the recent studies by Huber and Vilgis[29] who modeled the Payne effect based on the cluster–cluster aggregation (CCA) model. They obtained $m = 1/(C - d_f + 2)$, where C is a connectivity exponent related to the minimum path along the cluster structure and d_f is the fractal dimension of clusters. Therefore, the fitting parameter m has a physical meaning related to filler structures or filler immobilized rubber structures (a reflection of filler structure). For DSF, the structure involving soy carbohydrate is more complicated and does not fit the description of the CCA model. However, an empirical fit is useful to show the difference in their strain behaviors (Fig. 11 and Table I) between the different composites. The model fit and standard deviation of the fit coefficients in Table I were based on 99.73% confidence level using Igor Pro 4.0 software. In general, a smaller fitting parameter m indicates a continuous decrease of G′ with increasing strain and suggests a smoother and continuous breaking up of filler network structure as the strain is increased. On the other hand, a larger m indicates a strong structure at lower strains, which does not yield until a certain strain is reached. A smaller γ_c value indicates that the filler related network structure is less elastic and breaks down substantially at smaller strains. From Figure 11 and Table I, the fitting using the Kraus model is generally acceptable except when a significant G′ maximum occurs in the small strain region. Not all the m values of the co-filler composites are within the range set by those of DSF and CB composites, indicating that filler related network structure varies with co-filler ratio and can not be easily extrapolated from their single filler composites. For both 20 and 30% single filler composites, m values are in the range of 0.7–0.9. For the co-filler composites, m values are in the range between 0.6 and 0.9. Both m and γ_c values from the composites prepared by the freeze-drying method are larger than that of DSF and CB single filler composites prepared by a casting method.[1] This again indicates that the composites prepared by freeze-drying method have a less brittle structure, likely due to the polymer mediation effect. In this aspect, the characteristic strain γ_c has a physical meaning associated with the brittleness of the composite structures. For the co-filler composites, it is also observed in Table I that γ_c decreases as the CB content is increased, indicating the filler network breaks down at a smaller strain as CB content increases in the composites. This may indicate that the filler network structure of co-filler composites is not as strong as that of the DSF composites at lower strains when more CB aggregates are incorporated into the co-filler network, which also implies weaker filler–filler interactions between DSF and CB aggregates. A similar trend is also observed in 20% co-filler composites (Table I). When comparing 30% co-filler composites with 20% co-filler composites, γ_c increases when the co-filler fraction is decreased and rubber fraction is increased (Table I). This is an indication that filler related network structures become more elastic when more rubber is incorporated, which causes the characteristic strain γ_c to shift to a larger strain.

TABLE I
Fitting Parameters for Shear Elastic Modulus Data[a]

Composition	Best fit[b] m	γ_c (%)	G_0' (MPa)	G_∞' (MPa)
30% single filler				
DSF	0.94 ± 0.09	1.69 ± 0.11	27.9 ± 0.19	11.4 ± 0.60
CB	0.72 ± 0.1	1.64 ± 0.19	5.84 ± 0.06	2.52 ± 0.18
30% Co-filler				
CB : DSF = 1 : 3	0.85 ± 0.12	1.76 ± 0.20	18.1 ± 0.13	9.12 ± 0.59
CB : DSF = 1 : 1	0.52 ± 0.03	0.72 ± 0.04	13.3 ± 0.06	7.39 ± 0.14
CB : DSF = 3 : 1	0.71 ± 0.13	0.64 ± 0.10	8.58 ± 0.10	5.26 ± 0.23
20% single filler				
DSF	0.90 ± 0.15	3.01 ± 0.35	7.99 ± 0.07	3.67 ± 0.28
CB	0.80 ± 0.17	3.36 ± 0.63	1.30 ± 0.01	0.94 ± 0.04
20% Co-filler				
CB : DSF = 1 : 3	0.90 ± 0.25	3.63 ± 0.77	2.36 ± 0.02	1.59 ± 0.10
CB : DSF = 1 : 1	0.76 ± 0.26	2.07 ± 0.65	3.28 ± 0.04	2.16 ± 0.19
CB : DSF = 3 : 1	0.59 ± 0.09	1.10 ± 0.16	2.54 ± 0.01	1.89 ± 0.04

[a] The data are from the 8th strain cycle measured at 140°C.
[b] Best fit of shear elastic modulus vs. strain with the Kraus Model.

CONCLUSIONS

At 140°C, a single filler composite filled with 30% DSF exhibited roughly a 230-fold increase in G′ compared with the unfilled SB rubber. Mixtures of DSF and CB at different ratios were used as co-fillers to reinforce carboxylated styrene-butadiene rubber composites. All composites were made by a freeze-drying and compression-molding method. Thermal mechanical measurements of G′ showed that DSF composites had a significantly greater G′ than CB composites within the rubber plateau region. Compared to CB composites, all co-filler composites showed a greater elastic modulus in the rubber plateau region. Although the composites with higher DSF content had a higher G′, the composites with higher CB content yielded a better recovery behavior. The composites with ~ 50% substitution of CB by DSF appeared to be a compromise and gave a balanced property between elastic modulus and recovery behavior. The Payne effect of DSF, CB, and co-filler composites at 140°C was interpreted using the Kraus model. The results indicated that the co-filler composites with a higher CB content had a weaker but more elastic filler network structure. This study demonstrated the use of DSF to partially substitute CB as reinforcement co-filler produced rubber composites with an enhanced shear modulus and reduced cost.

The author thanks various industrial companies mentioned in the materials section for supplying materials used in this study, and Dr. S. C. Peterson for proofreading this manuscript.

References

1. Jong, L. J Appl Polym Sci 2005, 98, 353.
2. Jong, L. Polym Int 2005, 54, 1572.
3. Jong, L. Compos A 2006, 37, 438.
4. Jong, L. J Polym Sci Part B: Polym Phys 2005, 43, 3503.
5. Ismail, H.; Jaffri, R. M.; Rozman, H. D. J Elastomers Plast 2003, 35, 181.
6. Nair, K. G.; Dufresne, A. Biomacromolecules 2003, 4, 666.
7. Ismail, H.; Shuhelmy, S.; Edyham, M. R. Eur Polym J 2001, 38, 39.
8. Coughlin, E. T. A. U.S. Pat. 2,056,958 (1936).
9. Isaacs, M. R. U.S. Pat. 2,127,298 (1938).
10. Lehmann, R. L.; Petusseau, B. J.; Pinazzi, C. P. U.S. Pat. 2,931,845 (1960).
11. Fuetterer, C. T. U.S. Pat. 3,113,605 (1963).
12. Beckmann, O.; Teves, R.; Loreth, W. Ger Offen DE 19,622,169 A1 19,961,212 (1996).
13. Recker, C. Eur. Pat. Appl. EP 1,234,852 A1 20,020,828 (2002).
14. Heinrich, G.; Kluppel, M. Adv Polym Sci 2002, 160, 1.
15. Wang, M. J. Rubber Chem Technol 1998, 71, 520.
16. Carter, C. M.; Cravens, W. W.; Horan, F. E.; Lewis, C. J.; Mattil, K. F.; Williams, L. D. In Protein Resources and Technology; Milnre, M.; Scrimshaw, N. S.; Wang, D. I. C., Eds.; AVI Publishing: Connecticut, 1978; Chapter 17.
17. Richard, J. Polymer 1992, 33, 562.
18. Zosel, A.; Ley, G. Macromolecules 1993, 26, 2222.
19. Kan, C. S.; Blackson, J. H. Macromolecules 1996, 29, 6853.
20. Garcia, M. C.; Torre, M.; Marina, M. L.; Laborda, F. Crit Rev Food Sci Nutr 1997, 37, 361.
21. Chazeau, L.; Brown, J. D.; Yanyo, L. C.; Sternstein, S. S. Polym Compos 2000, 21, 202.
22. Yurekli, K.; Krishnamoorti, R.; Tse, M. F.; Mcelrath, K. O.; Tsou, A. H.; Wang, H. C. J Polym Sci Part B: Polym Phys 2001, 39, 256.
23. Vieweg, S.; Unger, R.; Hempel, E.; Donth, E. J Non-Cryst Solids 1998, 235/237, 470.
24. Payne, A. R. J Appl Polym Sci 1962, 6, 57.
25. Payne, A. R. J Appl Polym Sci 1962, 6, 368.
26. Payne, A. R. J Appl Polym Sci 1963, 7, 873.
27. Kraus, G. J Polym Sci Polym Symp 1984, 39, 75.
28. Ulmer, J. D. Rubber Chem Technol 1995, 69, 15.
29. Huber, G.; Vilgis, T. A. Kautsch Gummi Kunstst 1999, 52, 102.